Materials and Structures (2014) 47:1205–1220
DOI 10.1617/s11527-013-0123-4

ORIGINAL ARTICLE

Laboratory investigation of bitumen based on round robin DSC and AFM tests

Hilde Soenen · Jeroen Besamusca · Hartmut R. Fischer · Lily D. Poulikakos · Jean-Pascal Planche · Prabir K. Das · Niki Kringos · James R. A. Grenfell · Xiaohu Lu · Emmanuel Chailleux

Received: 14 March 2013 / Accepted: 8 June 2013 / Published online: 21 June 2013

Abstract In the past years a wide discussion has been held among asphalt researchers regarding the existence and interpretation of observed microstructures on bitumen surfaces. To investigate this, the RILEM technical committee on nano bituminous materials 231-NBM has conducted a round robin study combining differential scanning calorimetry (DSC) and Atomic Force Microscopy (AFM). From this, methods for performing DSC and AFM tests on bitumen samples and determination of the influence of wax on the observed phases, taking into account thermal history, sample preparation and annealing procedure, are presented and critically discussed. DSC is used to measure various properties and phenomena that indicate physical changes such as glass transition temperature (T_g) and phase transition such as melting and crystallization. In the case of existence of wax, either natural or synthetic, it can further indicate the melting point of wax, that could be used to determine wax content. The results from seven laboratories show

H. Soenen
Nynas NV, Noorderlaan 183, 2030 Antwerpen, Belgium
e-mail: hilde.soenen@nynas.com

J. Besamusca
Kuwait Petroleum Research and Technology,
Moezelweg 251, Europoort (Rt), The Netherlands
e-mail: j.besamusca@Q8.com

H. R. Fischer
TNO, Technical Sciences, De Rondom 1,
5612 AP Eindhoven, The Netherlands
e-mail: hartmut.fischer@tno.nl

L. D. Poulikakos (✉)
Empa, Swiss Federal Laboratories for Materials Science and Technology, Überlandstrasse 129, 8600 Dübendorf, Switzerland
e-mail: Lily.poulikakos@empa.ch

J.-P. Planche
Western Research Institute, 365 North 9th Street,
Laramie, WY 82072, USA
e-mail: jplanche@uwyo.edu

P. K. Das · N. Kringos
Division of Highway and Railway Engineering, KTH Royal Institute of Technology, 10044 Stockholm, Sweden
e-mail: prabir.kumar@abe.kth.se

N. Kringos
e-mail: Kringos@kth.se

J. R. A. Grenfell
Nottingham Transportation Engineering Centre,
University of Nottingham, University Park,
Nottingham NG7 2RD, UK
e-mail: James.Grenfell@nottingham.ac.uk

X. Lu
Nynas, Nynas AB, 149 82 Nynäshamn, Sweden
e-mail: xiaohu.lu@nynas.com

E. Chailleux
IFSTTAR, Versailles, France
e-mail: emmanuel.chailleux@ifsttar.fr

that T_g temperatures obtained from the heating scans are more repeatable and easier to obtain in comparison to the cooling scans. No significant difference was noted for T_g's obtained from the first and second heating scans. AFM is an imaging tool used to characterize the microstructures on a bituminous surface. Using AFM three phases in the materials with wax could be distinguished. The changes in the phases observed with AFM for increases in temperature were correlated with the DSC curve, and it could be established that the so called "Bee" structure disappeared around the melting peak in the DSC curve. Thus, this research has confirmed the relation between the microstructures on a bitumen surface and the wax content.

Keywords Bitumen · Asphalt · DSC · AFM · Wax · Multiphase material

1 Introduction and motivation

Differential scanning calorimetry (DSC) is a thermo-analytical method that allows the determination of physical changes in a material associated with a heat exchange. DSC has shown promising results in analyzing bitumen as it can be used to measure various properties and phenomena in the material. The properties that are especially relevant for bitumen are physical changes such as glass transition temperature (T_g) and phase transition such as melting and crystallization. Furthermore, chemical reactions and heat capacity can be measured [1, 2]. In case of the existence of wax in bitumen it can further indicate the melting point of wax and the results could be used to determine wax content [3].

Atomic force microscopy (AFM) is an imaging tool that delivers information on the topography and phase contrast of the sample surface and is particularly useful for multi-phase materials such as bitumen. The advantage of AFM is that it requires relatively simple sample preparation and operates under ambient conditions. Recently developed imaging techniques also allow the imaging of the dynamic interaction of the probe tip with the substrate material. In that case, in addition the probe is actuated and the damping of the vibrations of the probe while being in close contact with the substrate is registered and used as a feed-back signal. Also and especially in case of sticky substrates like bitumen, the difference in phase of the actuated vibration and of the registered response, the phase signal, can indicate areas which differ in stiffness and tackiness. Such phase images along with topography images of bitumen surface indicate that this composite material is not a perfectly homogeneous mixture of hydrocarbons and that not all the hydrocarbons are mutually soluble at room temperature. Previous research has shown that the wax in bitumen, if present, can appear in the form of a type of a "Bee" structure with three identifiable phases [4–11]. This point will be further discussed in Sect. 4.

The disadvantage of AFM is that it delivers surface images only and for that it needs a relatively smooth surface. Therefore, one should be aware that the sample preparation could influence what is measured at the surface, and that surface properties are not always reflective of bulk properties.

Natural wax in petroleum is often defined as the material that precipitates at a certain temperature or upon cooling. Two types of wax have been identified in bitumen: paraffin wax and micro-crystalline wax. Paraffin wax refers to the group of n-alkanes with few or no branches (C20–C40). Micro-crystalline wax, on the other hand, is collected in the residue or in the bitumen fraction after the distillation process and mainly consists of naphthens and iso-paraffins [12, 13]. Both types of wax can be visualized using AFM. Paraffin wax crystalizes in large flat plates or needles and is also known as macro-crystalline wax. The micro-crystalline wax, in contrast, consists of aliphatic hydrocarbons with a higher boiling point and crystallizes as small microscopic needles [11, 17]. Using bitumen with natural wax Lu and Redelius [13] have shown testing bitumen with specific wax contents, that the rheological properties at high service temperatures were not influenced by wax content. However, at low temperature the presence of wax in bitumen resulted in physical hardening of waxy bitumens and in turn resulted in asphalt mixtures with higher fracture temperature. The effects of time, temperature and thermal cycling on wax crystallization in bitumen were studied using various characterization techniques. It was shown that non-waxy bitumens displayed no crystal structure. It was possible to show that the morphology of the crystals was highly dependent on crystallization temperature and temperature history. The investigated samples

indicated that bitumen wax usually melted at temperatures lower than 60 °C [11]. Planche et al. have shown that at low temperatures, crystallized fraction(s) (CFs) seem greatly responsible for the physical hardening (PH) occurring with time. PH magnitude also depends on the position of T_g relative to the given conditioning temperature. At higher temperatures, CF also plays a role on the rheological behavior since their dissolution-precipitation mainly occurs at temperatures between 0° and 80 °C [14]. The same team has also shown using Phase Contrast Microscopy, that the presence of wax in bitumen can lead to the phase separation of a single homogeneous liquid into two liquid phases upon cooling through a spinodal decomposition [22],

Waxes isolated from different bitumens were investigated with respect to their chemical compositions and structural characteristics. The composition of the waxes was strongly influenced by the origin as well as the separation methods [15]. Furthermore, Michon et al. [16] have reported that depending on the annealing procedure and heating and cooling rate different DSC thermograms are obtained that in turn can result in different endothermic peaks used to calculate the wax content.

As discussed above, the use of DSC and AFM have shown to be promising for the characterization of bituminous materials. Therefore, the RILEM technical committee (TC) on nano bituminous materials 231-NBM has conducted a round robin study focusing on combining the information from these two test methods. The main objective of this paper is to present the results of the round robin tests using DSC and AFM on bitumen samples taking into account thermal history and annealing procedure. Eight laboratories participated in various aspects of this study seven from Europe and one from the United States. The participating laboratories were Kuwait Petroleum Research & Technology (Q8), Nynas, KTH Royal Institute of Technology, IFSTTAR, Empa, Swiss Federal Laboratories for Materials Science and Technology, University of Nottingham, Western Research Institute and TNO Technical Sciences with the lab numbering presented in this order.

Table 2 Result of SARA tests for the tested bitumen (Courtesy Nynas)

	Bit A	Bit B	Bit C	Bit D
Saturates	6.4	7.3	3.8	6.1
Aromatics	48.6	53.2	59.6	48.7
Resins	26.2	20.3	22.2	23.8
Asphaltenes	18.8	19.2	14.6	21.4

2 Materials

In this investigation four types of bitumens were selected based on their expected wax content with designations Bit-A, Bit-B, Bit-C and Bit-D. Table 1 lists the standard physical material properties provided by the suppliers who are members of the TC. Bit-A

Table 1 Standard material properties

Designation	Source	Bitumen	Pen (0.1 mm)	Soft. Point (°C)	DSC[c] wax (%)	EN wax (%)	Dyn. Viscosity @ 60C Pa s	Kin. Viscosity @ 135C (mm^2/s)	Fraass breaking point (°C)
Bit-A	Venezuela	70/100	91	46.2	0	0 3[a,b]	168[a]	342[a]	−15[a]
Bit-B	NN	70/100	86	46.4	6.2	1.7	96	181	−16
Bit-C	Kuwait Export Crude	70/100	82	45.8	NN	1	163	399	−15
Bit-D	Venezuela	70/100 Wax mod	50	78	4.5	NN	NN	257	−14

NN Not Known

[a] Average values not on exactly the same sample

[b] Using the EN method, some wax content is obtained even for non-waxy bitumen

[c] For natural wax 121 J/g and for synthetic wax 250 J/g was used to calculate wax %

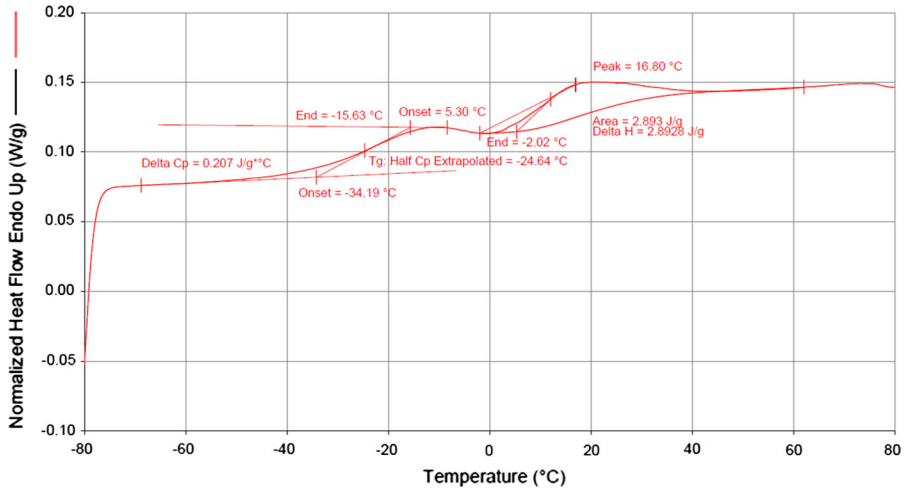

Fig. 1 Example of the relevant temperatures from DSC results of the second heating scan for Bit-C also shown in Table 3 where $T_m = T_g$ and Peak $= T_{pm}$, with corresponding onset and end temperatures (plot courtesy of Lab5)

contains no wax, Bit-B and Bit-C contain natural wax whereas Bit-D is Bit-A that is doped with 3 % synthetic wax (Sasobit 1596). Addition of this wax decreased the penetration level at 25 °C and increased the softening point, as seen in the values for Bit-A in comparison with Bit-D shown in Table 1. Measurement of the wax fraction can differ depending on method used. As shown in Table 1 the wax content using EN 12606 [18] can be quite different in comparison to the wax content using a method based on DSC [3]. The wax content shown in Table 1 using DSC was calculated from the endothermic peak during the heating scan, and a constant melting enthalpy of 121 J/g used as reference. This wax content can vary as other labs have used a melting enthalpy of 200 J/g. In the round robin tests wax percentage was not calculated.

Thin layer chromatography-flame ionization detector, Iatroscan (TLC-FID) was used to determine SARA fractions (saturates, aromatics, resins and asphaltenes) of the various bitumen. Results are presented in Table 2. The tests were performed using a procedure similar to the standard method (IP-469). Comparing Bit-A and Bit-D, it seems that the synthetic wax is determined as part of the asphaltene fraction.

3 Methods

3.1 Existing standards

Various international standards such as ISO and ASTM are used for DSC [1, 2, 19]. The test methods describe the determination of the glass transition, melting and crystallization temperatures of polymeric materials using DSC or differential thermal analysis. The methods are applicable to amorphous materials or to partially crystalline materials containing amorphous regions, that are stable and do not undergo decomposition or sublimation in the glass transition region. The operating temperature range, according to these standards, is from −120 to 500 °C [2]. Figure 1 and Table 3 show schematically the definition of the relevant temperatures around glass transition temperature and the melting peak obtained from the DSC

Table 3 Definition of temperatures, all in °C (after ASTM [2, 3])

Designation	Definition
Temperatures related to a glass transition	
T_0	Temperature of first baseline deviation
T_f	Extrapolated onset temperature
T_m	Midpoint temperature, also referred to as glass transition temperature T_g
T_i	Inflection temperature
T_e	Extrapolated end temperature
T_r	Temperature of return to baseline
Temperatures related to melting and crystallization	
T_{eim}	Melting extrapolated onset
T_{efm}	Melting extrapolated end
T_{pm}	Melting peak temperature
T_{eic}	Crystallization extrapolated onset temperature
T_{efc}	Crystallization extrapolated end
T_{pc}	Crystallization peak temperature

thermograms. According to these definitions, T_m is usually used as the glass transition temperature T_g. Similarly a melting or crystallization peak can occur for bitumen with wax.

3.2 DSC procedure

3.2.1 Sample preparation, and conditioning (annealing)

Since bitumen shows aging due to oxidation and/or steric hardening, the sample preparation as well as the extraction of a representative sample out of bulk material needs attention. Using material from the top of a can is not recommended as more aging occurs at the surface. For these tests, approximately 15 mg of bitumen is placed in a DSC cup that is sealed with a lid with a small hole to prevent pressure build up and possible deformation of the cup during the test. The labs in this round robin tests have mostly used about 15 mg. However, this depends on the sample holder as too much bitumen mass can result in sample bubbling out of the sample holder during the experiment at higher temperatures. One lab has used ca. 6 mg. The sample was allowed to level out on the bottom of the cup by placing the cup horizontally for 15 min on a hot plate at about 110–130 °C. A proper contact between the bottom surface of the cup and the binder is needed; if the contact is not made, the onset of flow of the binder may give a signal in the DSC curve and create artifacts that are not due to any physical changes to the binder but geometric changes. Thereafter, the DSC cups are conditioned at 25 °C for 24–26 h horizontally for the annealing process.

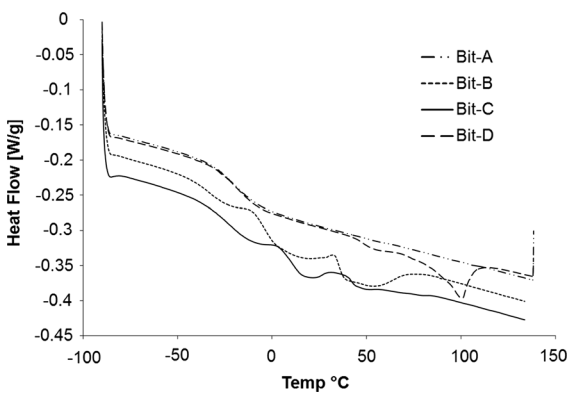

Fig. 2 Sample of results (Lab 7) from the 1st heating curve for the four bitumen tested, showing overlap of the T_g (*ca* −19 °C) for Bit-A and Bit-D. Bit-A does not show any melting signal

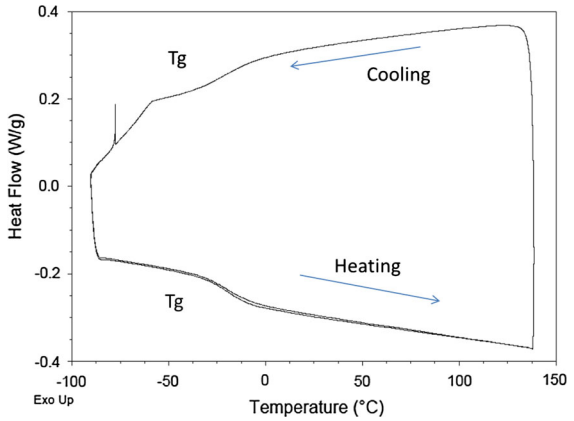

Fig. 3 Example of DSC curve for Bit-A shows no melting peak as it contains no wax but shows a clear T_g, both in the cooling scan and the two heating scans (plot courtesy of lab 7)

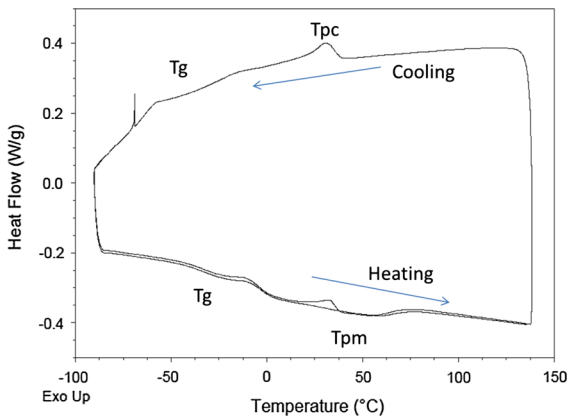

Fig. 4 Example of DSC curve for Bit-B with natural wax shows T_g, T_{pm} and T_{pc} (plot courtesy of lab 7)

3.2.2 Testing

The sample was placed in the DSC apparatus and conditioned at 25 °C for 5 min. Then it was cooled from 25 °C to at least –80 °C at −10 °C/min where it was left for 5 min isotherm at low temperature. The measurement phase was started at −80 to 140 °C also at 10 °C/min followed by cooling measurements from 140 °C down to −80 °C. After this cooling period, the sample was left for 5 min isothermally at −80 °C, followed by a

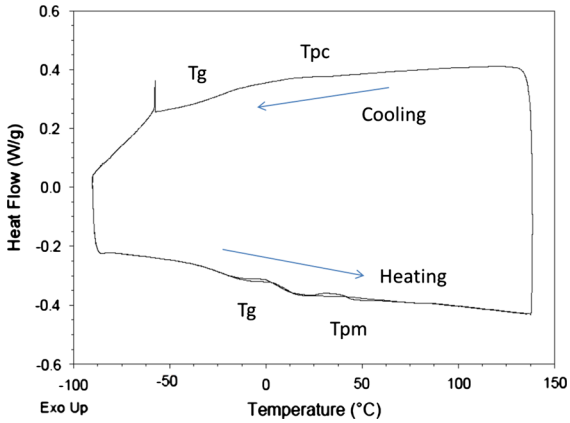

Fig. 5 Example of DSC curve for Bit-C with natural wax shows T_g and T_{pc}. T_{pm} was more difficult to identify due to a lack of a clear peak (plot courtesy of lab 7)

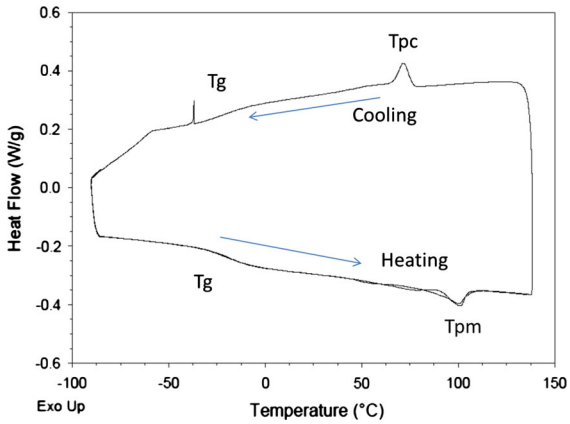

Fig. 6 Example of DSC curve for Bit-D with synthetic wax shows T_g, T_{pm} and T_{pc} clearly (plot courtesy of lab 7)

second heating measurement from the low temperature of −80 °C to 140 °C at a heating rate of 10 °C/min.

3.3 AFM procedure

3.3.1 Sample preparation and conditioning

As with DSC, assuring a representative sample out of bulk material and a sample preparation procedure to assure minimum aging needs attention. Bitumen as a binder will also collect dust or other airborne particles with time if not stored in a dust free environment. These particle contaminations may collect, especially at the surface and will hence disturb/alter the surface pattern as observable by AFM. Attention should be paid, that a sufficient thickness of the sample (100–500 μm) is left over to exclude surface driven and directed structuring effects [20] however, it should be noted that this is a somewhat thicker sample than is found in pavements.

One of the methods for AFM sample preparation is spin casting [5]. This type of sample is produced by dissolving bitumen in a solvent after which it is cast on a spinning plate. The centrifugal forces of the spinning plate spread the solution evenly and after evaporation of the solvent the resulting film thickness is in the nano- to micrometer range depending on the bitumen concentration in solvent. It was shown by Pauli et al. [5] that the number and size of the microstructural phases can change with respect to film thickness when thickness is decreased to a few nanometers. From hundreds of samples prepared in various ways, the same authors also found no evidence that the spin casting process has a significant effect upon the structures viewed on an asphalt surface using AFM. Thus, they found no solvent and aging effects: the solvent used has a similar effect in terms of asphalt component solubility to the temperature involved in the more classical way described below, and aging at the surface undergoes at the same rate regardless of the sample thickness. However, this sample preparation technique is more complicated than the round robin method and as the goal here was to follow the sample preparation used in the DSC tests it was not used in these round robin procedures. Section 4 presents a sample of AFM images using spin casting.

The method used in this investigation follows the DSC testing procedure closely. For this procedure approximately 15 mg of binder is placed in a conductive sample holder. The sample holder is placed horizontally on a hot plate, 110–130 °C to let the binder level out for 15 min. Thereafter, the sample holder is left horizontally and covered to prevent dust pick-up, for at least 24–26 h, at 25 °C prior to carrying out the tests.

3.3.2 Testing

The testing procedure also follows the DSC procedure closely as the microstructure that forms on the sample surface is dependent on its thermal history. The tests can be conducted at variable temperatures or at constant temperature. The sample is placed in the AFM apparatus and conditioned at 25 °C for 5 min. Then it was

Table 4 Average and standard deviation (S) of glass transition temperatures per binder type (all labs are included)

Sample	DSC run	T_f, °C		T_m, °C		T_e, °C	
		Average	S	Average	S	Average	S
Bit A	1st heating	−30.8	5.7	−19.0	1.2	−5.4	5.8
	2nd heating	−30.5	5.2	−17.8	1.3	−5.3	5.4
	Cooling	−25.2	15.3	−27.5	9.6	-31.0	14.1
Bit B	1st heating	−41.0	2.0	−31.4	4.0	−21.9	7.2
	2nd heating	−41.0	2.5	−30.0	4.2	−20.0	7.9
	Cooling	−37.5	19.6	−39.6	13.6	−41.6	13.7
Bit C	1st heating	−34.0	3.0	−22.0	3.2	−7.6	8.6
	2nd heating	−35.3	2.9	−23.8	3.9	−13.3	5.5
	Cooling	−16.9	18.6	−25.4	10.9	−25.9	20.5
Bit D	1st heating	−27.6	8.1	−16.4	2.1	−2.9	7.2
	2nd heating	−29.6	9.3	−18.1	1.3	−2.5	6.4
	Cooling	−13.8	32.1	−18.7	19.7	−31.6	12.4

cooled from 25 °C to –30 °C at −10 °C/min where it was left for 5 min at this isothermal temperature. The measurement phase starts at −30 °C. However, special attention is needed here since ice formation due to condensation of humidity of the air may occur. This can be prevented by a flow of dry nitrogen gas keeping in mind that the flow velocity must be small not to disturb the measurement. In order to avoid this, it is recommended to start the imaging at 0 °C in case variable temperature capability is available. Further images may be taken, depending on the thermal features recorded by DSC at 0 °C, 15 °C, 25 °C and thereafter at 5 °C intervals (i.e., 30 °C, 35 °C, 40 °C, 45 °C …) until no micro-structure is observable. For AFM imaging of bitumen stiff cantilevers (∼40 N/m) are used operating

Table 5 Individual glass transition temperatures per lab and per binder type (T_m taken from the first heating scan)

	T_m (°C) (first heating)			
	Bit-A	Bit-B	Bit-C	Bit-D
lab-1	−17.3	−34.0	−22.6	−16.5
lab-2	−18.4	−33.0	−24.0	−18.6
lab-3	−20.1	−26.3	−21.8	−18.4
lab-4	−19.8	−32.5	−20.9	−14.7
lab-5	−19.5	−33.2	−23.3	−17.3
lab-6	−19.4	−34.1	−24.8	−12.8
lab-7	−20.8	−24.0	−14.0	−14.5
Average	−19.3	−31.0	−21.6	−16.1

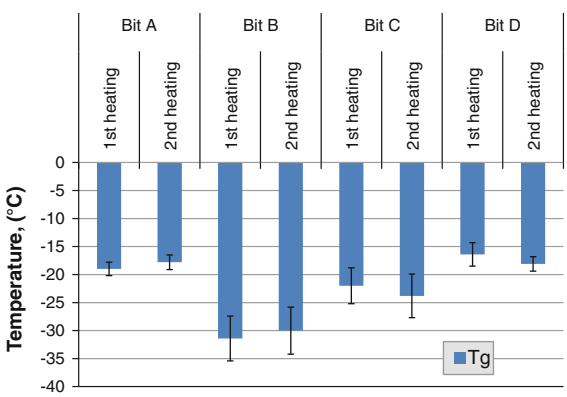

Fig. 7 Overview of average T_g midpoint temperatures, determined for all binders from first and second heating scans. The standard deviation is half the length of the total error bar

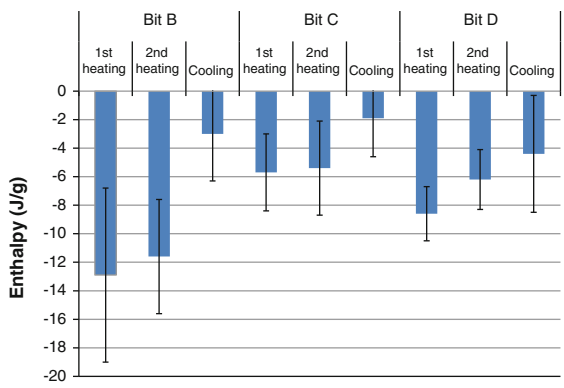

Fig. 8 Average melting and crystallization enthalpies for seven labs, determined in the first and second heating scan and upon cooling. The standard deviation is half the total length of the error bar

Table 6 Average and standard deviation (S) of melting and crystallization enthalpies (all labs are included)

Sample	DSC run	Enthalpy, J/g		
		Average	*S*	*S*/average, %
Bit B	1st heating	−12.9	6.1	47
	2nd heating	−11.6	4.0	35
	Cooling	−3.0	3.3	112
Bit C	1st heating	−5.7	2.7	48
	2nd heating	−5.4	3.3	62
	Cooling	−1.9	2.7	143
Bit D	1st heating	−8.6	1.9	22
	2nd heating	−6.2	2.1	35
	Cooling	−4.4	4.1	93

in the TappingMode™ at resonance frequencies of 300 kHz with a minimum of damping of the amplitude signal. AFM Temperature monitoring is device dependent in the case of Lab 5, 1000 Ω platinum resistance temperature detector (RTD) is used which is bonded to one of the puck hold-down clips with the conductive sample holder.

4 Results and discussion

4.1 DSC

The method registers the difference in the rate of heat flow into a specimen crucible or cup containing the specimen and that into a reference crucible as a function of temperature or time. In order to evaluate the transitions accurately, a temperature scan over a wide temperature range is needed; i.e. well before and well after the expected changes in the baseline. When a reduced temperature range is used, for example start of measurement at a rather high temperature, the baseline before the glass transition becomes very short and results in inaccurate T_g. If the tests are not conducted at high enough temperatures, part of the melting signal can be missed. As discussed in Sect. 3 the DSC temperature range used here is at least −80 °C to 140 °C. The proper temperature range can vary depending on the type of bitumen; however this range was sufficient for the materials used here. Challenges faced in performing these tests are discussed elsewhere [21].

4.1.1 Evaluation of glass transition temperature T_g

The bitumen used in sample A and D are derived from the same crude origin and show similar T_g values. Bit-B and Bit-C are from different origins and show different T_g values (Fig. 2). Sample of DSC curves from Lab 7 for all the investigated binders are shown in Figs. 3, 4, 5 and. 6. As seen in these figures T_g can be identified from a shift in the baseline. Summary of the results shown in Table 4 and Fig. 7 indicate that there is good reproducibility of T_g temperatures. The reproducibility of T_g for Bit-A and Bit-D (standard deviation, S, on T_m was 1.9 °C and 2.1 °C respectively) was better

Table 7 Average and standard deviation (S) of melting and crystallization temperatures from seven labs

Sample	DSC scan	Tpm peak		Teim extrap. onset		Tefm extrap. end	
		Average	*S*	Average	*S*	Average	*S*
Bit-B	1st heating	51.8	2.8	0.1	14.4	91.0	17.5
	2nd heating	52.2	6.6	0.1	13.2	98.3	23.4
Bit-C	1st heating	28.1	13.7	6.9	5.2	98.2	16.8
	2nd heating	21.8	2.7	4.4	4.3	87.2	26.3
Bit-D	1st heating	100.6	1.4	51.2	27.4	119.6	7.4
	2nd heating	101.4	0.9	55.4	30.5	117.7	8.2
		Tpc peak		Teic extrap. onset		Tefc extrap. end	
		Average	*S*	Average	*S*	Average	*S*
Bit-B	Cooling	31.3	1.5	42.9	5.5	8.1	11.1
Bit-C	Cooling	19.9	10.0	43.5	33.3	9.8	20.8
Bit-D	Cooling	71.6	3.0	73.0	25.6	40.4	33.8

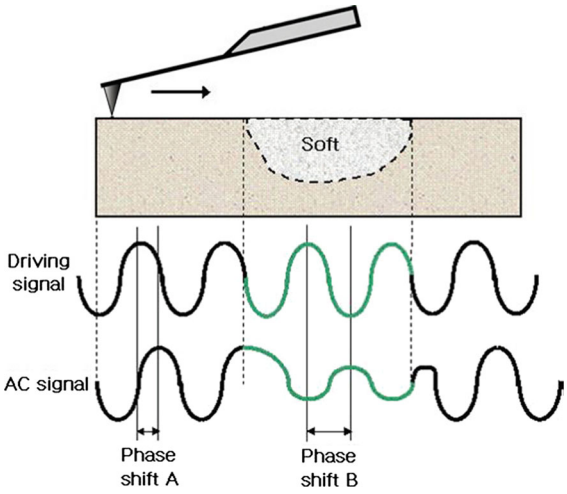

Fig. 9 The phase lag is monitored while the topographic image is being taken so that images of topography and material properties can be collected simultaneously [Park AFM information bulletin http://www.parkafm.com/AFM]

compared to bitumen with natural wax (Bit-B and Bit-C) (S on T_m was 4.0 °C and 3.2 °C). This is due to the fact that one of the required temperatures, the extrapolated end temperature, T_e becomes difficult to determine, due to an overlap with recrystallization and melting phenomena. It is also clear from Fig. 7 that for the investigated bitumens there is no significant difference between the first and the second heating scans. Adding synthetic wax (3 %) did not change the T_g value as shown in Fig. 7 and Table 4; the T_g values of Bit-A and Bit-D are similar. Conditioning for 24 h at 25 °C (annealing before heating 1) did not significantly change T_g values compared to values without conditioning (heating 2). The results presented here indicate that T_g temperatures obtained from the cooling scans were very often complicated due to the occurrence of small spikes (or peaks) appearing in the curves for some labs (cf. Figs. 3, 4, 5, and 6). These were attributed to differences in contraction properties of

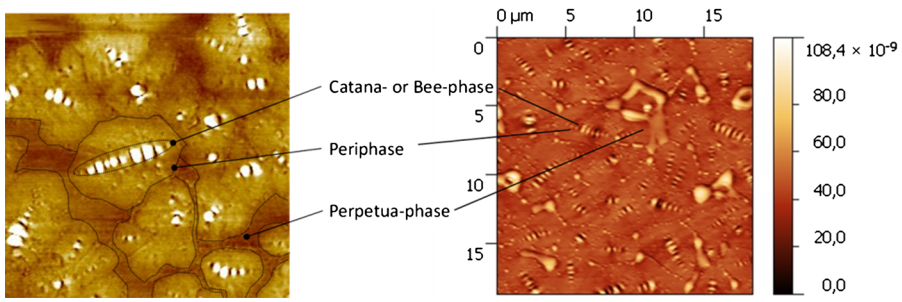

Fig. 10 Identification of three phases in the microstructure of Bit-C using AFM (scale of left figure is 10 × 10 µm) showing phase contrast left and topography right, The left picture shows a freshly prepared sample, the right picture shows the same sample aged at room temperature for about 3 weeks (courtesy Lab 8)

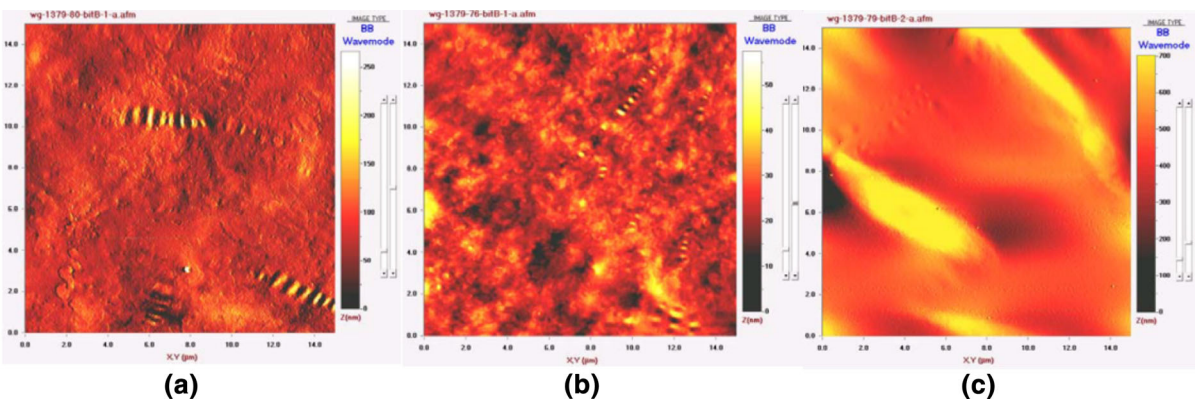

Fig. 11 AFM topography images of Bit-B using various sample preparation techniques: (a) spin cast rapid cooling, (b) hot plate smear rapid cooling and (c) hot plate smear slow cooling, image size 15 µm × 15 µm (images: courtesy Lab 7)

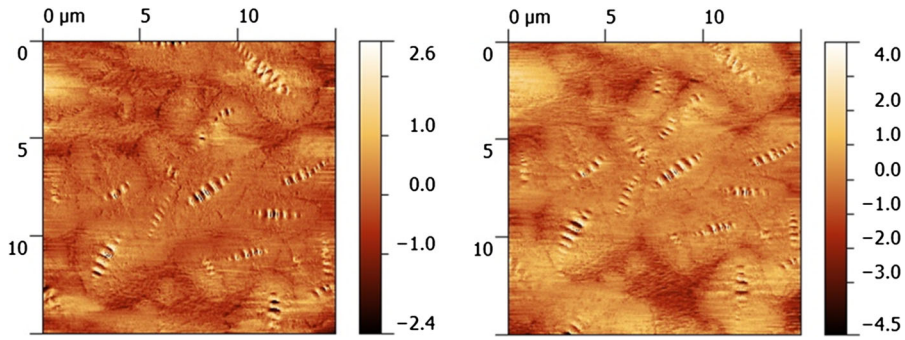

Fig. 12 Low temperature AFM phase contrast images of Bit-C: 0 °C left and 10 °C right (courtesy Lab 8)

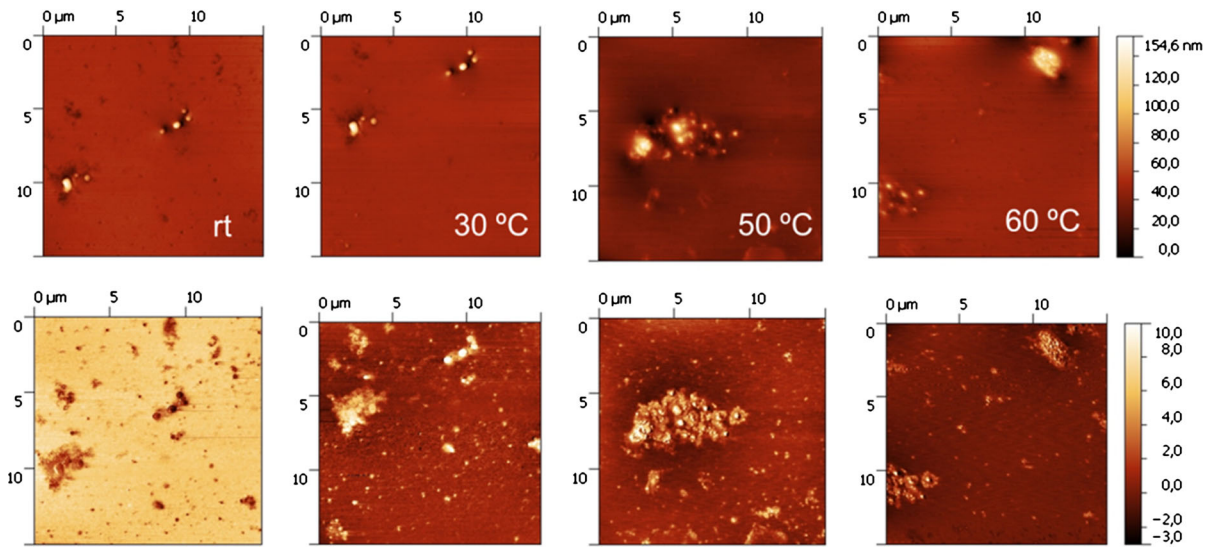

Fig. 13 AFM images showing topography, top and phase, bottom of Bit-A as a function of temperature, image size 15 µm × 15 µm (*rt* room temp, images: courtesy Lab 8)

bitumen and aluminum, resulting in loss of contact between the sample and the aluminum or sample cracking creating a spike in the heat flow curve.

As additional information, individual T_g mid temperatures, recorded from the first heating scan, are reported in Table 5 for each binder. The values for lab-1 and lab-2 are average values of the two repeats that were conducted by these labs. For the other labs, no repeats were available. None of the labs showed a systematic deviation from the average, however two data points, binder B and binder C, recorded by lab-7 could be seen as outliers when conducting a statistical analysis like Mandel h analysis or the Grubbs test. In this analysis both points were still included.

4.1.2 Evaluation of melting and crystallization enthalpies and wax content

In this round robin test, melting and crystallization enthalpies were derived from the DSC scans. A wax content, expressed in percentage was not calculated, since the enthalpy of a perfect 100 % crystalline material is not known, and it is not clear if the same value can be applied to all bitumen. However, only in Table 1, a percentage was calculated using a theoretical value of 121 J/g.

Figure 8 and Table 6 show values for each lab, averages and standard deviations (S) of melting enthalpies. It can be seen that the reproducibility of the enthalpy for the binder with synthetic wax (Bit-D)

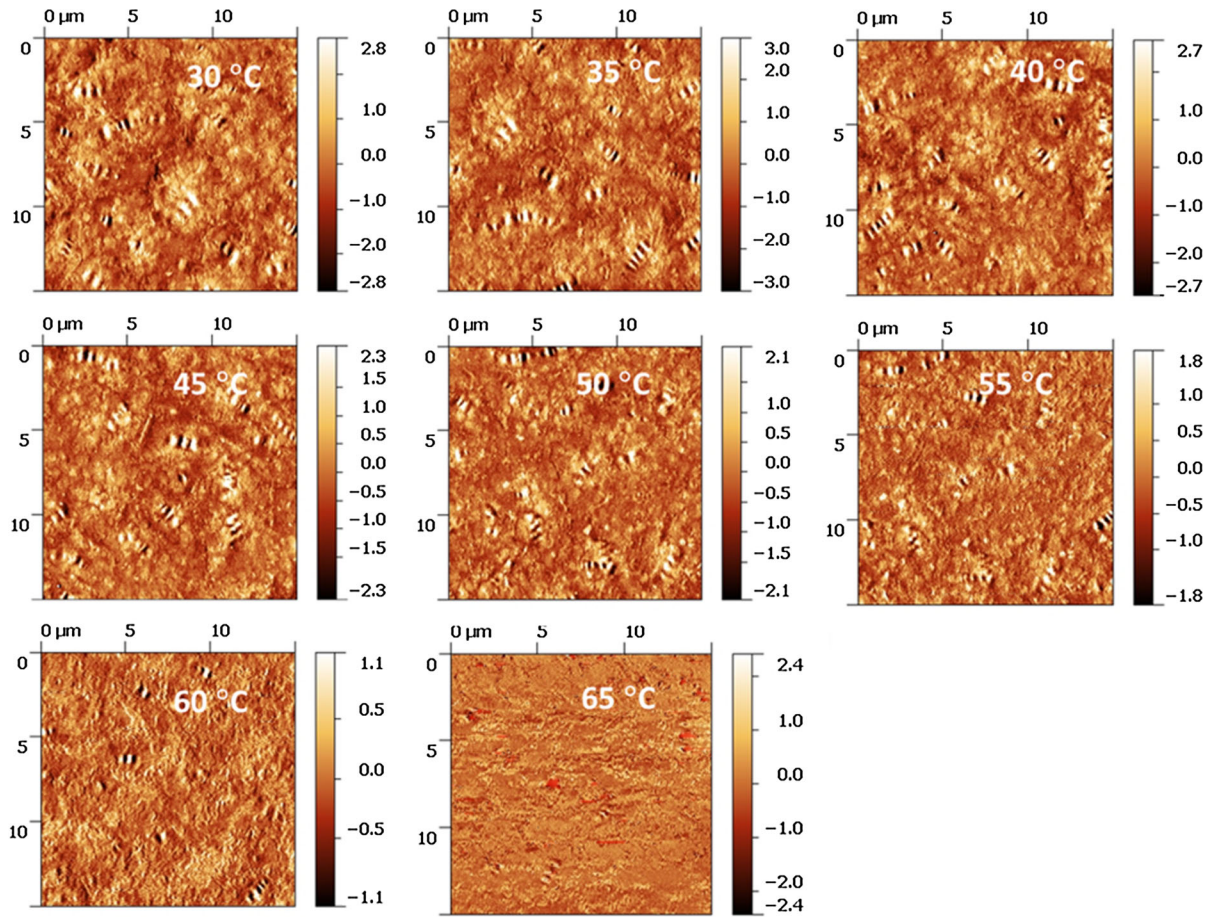

Fig. 14 AFM images showing phase contrast images of Bit-B as a function of temperature, image size 15 µm × 15 µm (images: courtesy Lab 8)

was better than those binders with natural wax (Bit-B and Bit-C). Standard deviation, S of the enthalpy from the first heating of Bit-B and Bit-C is almost 50 %, while it is 22 % for Bit-D. This can be attributed to baseline uncertainties and the fact that T_g is close to T_{eim} and T_{efc}. No significant difference in enthalpy value between 1st and 2nd heating was observed, but there is a clear difference in the shape of the curves which are thermal history dependent (Figs. 3, 4, 5, 6). Additionally, as discussed above, spikes in the cooling curves were observed that can be attributed to differences in contraction of bitumen and aluminum.

Enthalpies of crystallization are smaller compared to melting enthalpies derived from the heating scan. The reproducibility on the enthalpies from heating scans is generally better compared to those from cooling scans.

As shown in Table 7 larger variations in comparison to T_g were observed between labs for melting temperature (T_{pm}) for both types of waxes. The standard deviation for the first heating curve was 2.8 °C, 13.7 °C and 1.4 °C for Bit-B, Bit-C and Bit-D respectively, with T_{pm} being different for the two natural waxes Bit-B, Bit-C (51.8 °C vs. 28.1 °C respectively) and 100.6 °C for Bit-D with synthetic wax.

Comparing the results of the first and second heating scans gives an indication on the influence of conditioning. Conditioning of bitumen at 25 °C is in the melting range of natural wax for example in the case of Bit-C. Results show that influence of conditioning at 25 °C on enthalpy is low as shown in Table 6, but there is an influence in the melting temperature (Table 7). After annealing bitumen containing natural waxes, two peak temperatures become visible in the heating scan,

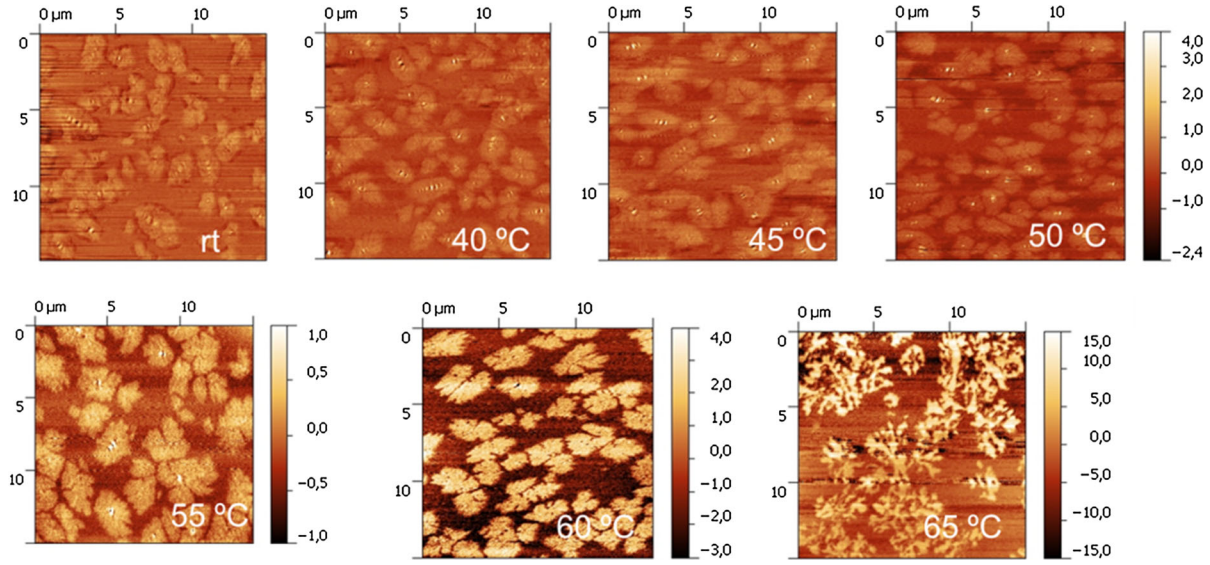

Fig. 15 AFM images showing phase contrast images of Bit-C as a function of temperature showing clearly the three phases of the material, image size 15 μm × 15 μm (*rt* room temp, images: courtesy Lab 8)

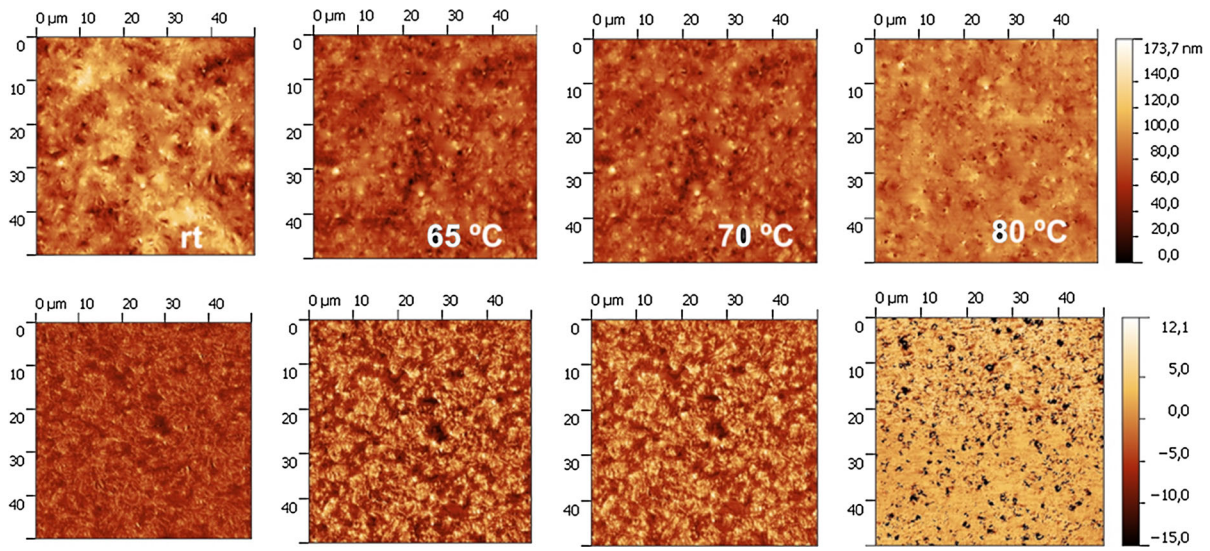

Fig. 16 AFM images showing topography, top and phase, bottom of Bit-D as a function of temperature image size 50 μm × 50 μm (*rt* room temp, images: courtesy Lab 8)

while this was not obvious after annealing the bitumen containing synthetic wax.

4.2 AFM

Phase Imaging, also referred to as phase detection microscopy (PDM), is another technique that can be used to map variations in surface properties such as elasticity, adhesion, and friction. It refers to the monitoring of the phase lag between the signal that drives the cantilever oscillation and the cantilever oscillation output signal, as shown in Fig. 9. Changes in the phase lag reflect changes in the mechanical properties of the sample surface. The phase lag is monitored while the topographic image is being taken so that images of topography and material properties

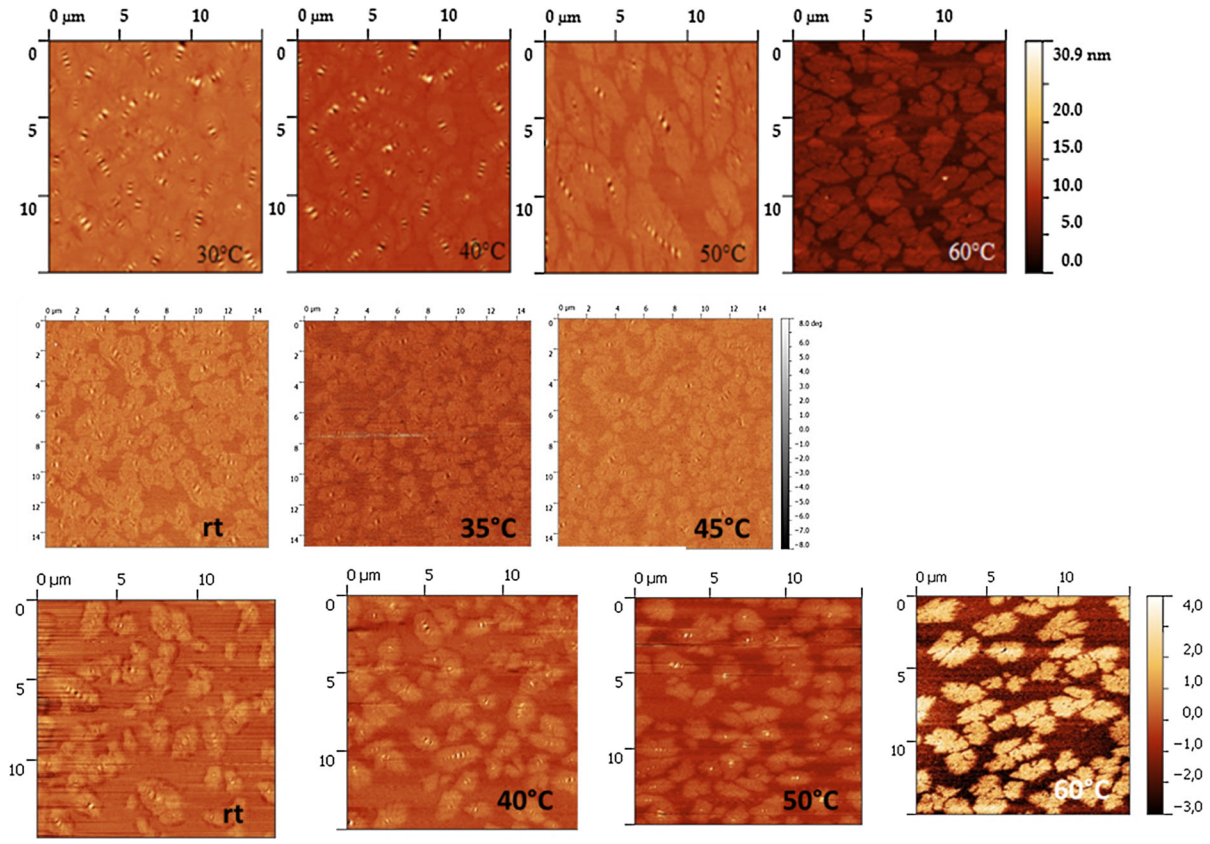

Fig. 17 AFM Comparative images from Bit C: *top* topography Lab 3, *middle* phase contrast Lab 5 and *bottom* phase contrast Lab 8, image size 15 µm × 15 µm (*rt* room temp)

can be collected simultaneously [Park AFM information bulletin, http://www.parkafm.com/AFM].

Various types of information were obtained from the AFM with phase contrast and topography as being the most commonly used source of information. AFM imaging resulted in the identification of three distinct phases shown in Fig. 10, namely the Catana or "Bee" structure as first phase, second the Periphase around the Catana and third the Perpetua phase [8–11]. Waxy, paraffinic material will crystallize or be frozen in the amorphous state during the cooling cycle depending on the cooling speed at the sample surface and, subsequently, non-crystalline parts (re)crystallize during the heating cycle when the temperature exceeds the glass-transition temperature (T_g). When the heating temperature reaches and exceeds the T_g region as during storage and annealing at ambient temperatures, the methylene groups of the *n*-alkane chains have sufficient mobility to rearrange to an all-*trans* conformation, which is a necessary condition for the onset of crystallization [16]. Consequently, very different images can be obtained depending on the preparation conditions and the time of isothermal aging or annealing. A melting/dissolution of the crystallites as observed by AFM is attributed to endotherm features (gradually melting) observable while performing thermal analysis such as DSC. Furthermore, as discussed in Sect. 3 thermal history, including sample preparation technique and thickness of the samples plays a direct role in the formation of the bitumen microstructure. Fig. 11 demonstrates this by showing Bit-B by (a) spin cast rapid cooling, (b) hot plate smear rapid cooling and (c) hot plate smear slow cooling. Therefore the round robin results presented here are from a uniform sample preparation and conditioning procedure. Effect of low temperature on the microstructure is demonstrated for Bit-C in Fig. 12. The three phases can be distinguished but a strong change in microstructure is absent.

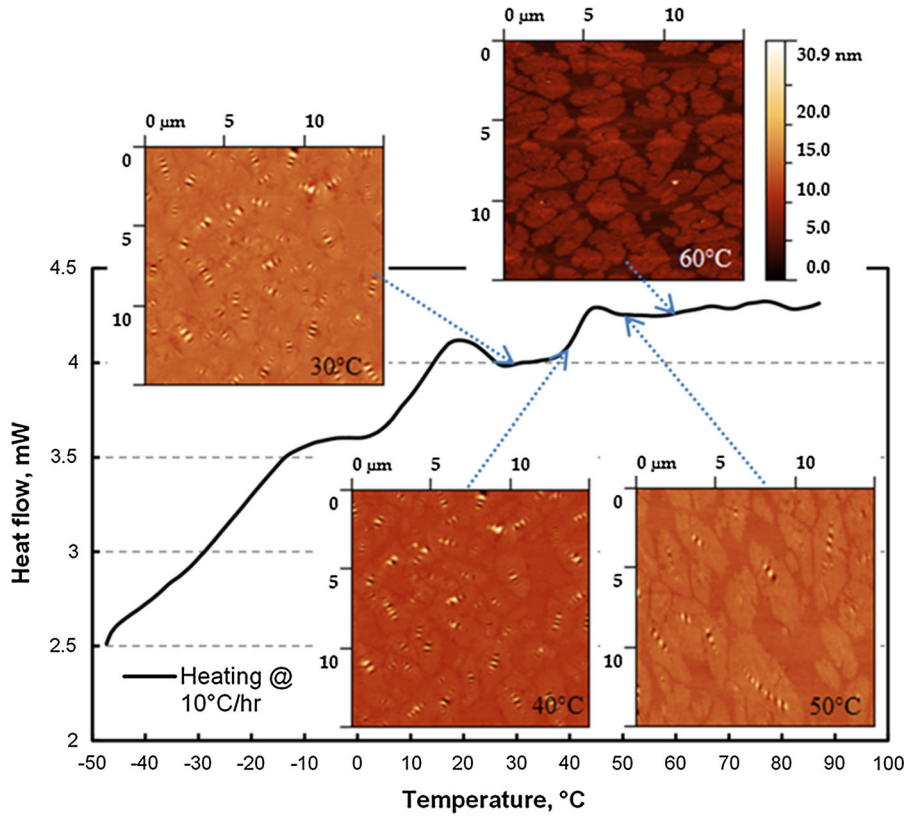

Fig. 18 AFM surface topography images of Bit-C as a function of temperature and corresponding DSC heating curve (images: courtesy Lab 3)

Figure 13, 14, 15, and 16 show AFM images of Bit-A, Bit-B, Bit-C and Bit-D respectively, showing topography, showing topography and/or phase contrast as a function of phase, bottom as a function of temperature. Bit-A contains no wax but displays some microstructure that can be attributed to flocculated asphaltenes. Comparing images of Bit-B with Bit-C (Figs. 14, 15) shows a different microstructure as well as response to temperature change that can be attributed to the difference in chemical compositions of the wax in Bit-B and Bit-C. Three labs in this round robin were capable of performing temperature related AFM. A sample of these results shown in Fig. 17 indicates that although a one to one comparison is difficult due to different contrast settings of the instruments, the tests show a change in the various phases with increase in temperature. Furthermore, it can be seen that the various phases are present to different degrees depending on the type of bitumen. The three phases of the material are most visible in Fig. 15 for Bit-C. Fig. 18 links the thermal events occurring upon heating as displayed by the DSC data such as glass transition (T_g) and melting peak temperature (T_{pm}) to the changes in microstructure for Bit-C.

Image analysis can provide additional information about the development of the areas covered by the different phases in time. For this, the phase angle signal of the images obtained at different temperatures were extracted from the images and plotted as area intensity against temperature by using 1D statistical functional

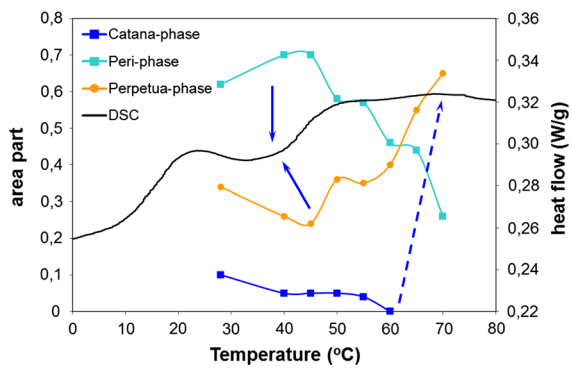

Fig. 19 Plot of the area in the AFM (15 × 15 µm^2) phase contrast pictures attributed to the different phases present within the microstructure of bitumen (Bit-C) and the corresponding DSC heating scan. (courtesy Lab 8) for color contrast the viewer is referred to the electronic version

analysis. A plot of the relative areas of the three distinguishable phases after deconvolution of the graphs representing areal intensity of the pixels with respect to temperature of the investigation is shown in Fig. 19 indicating the area in the AFM phase contrast pictures attributed to the different phases present within the microstructure that forms on the surface of bitumen (Bit-C) and the corresponding DSC heating scan. The change in area contribution of the different phases indicates clearly the transformations taking place in the bitumen as a function of temperature. The change in the phases with increase in temperature for a 15 μm × 15 μm area was correlated with the DSC curve and it could be established that the so called Bee structure disappeared around the second melting peak in the DSC curve. The arrows show recrystallization and increase in peri phase together with decrease in perpetua phase and the dashed arrow indicates melting connected with vanishing of catana phase, a strong decrease in peri and increase of perpetua phase area.

Challenges faced in performing these tests are discussed elsewhere [7]

5 Conclusions

The round robin experiments for DSC and AFM conducted by the Rilem TC 231-NBM in which eight laboratories seven from Europe and one from USA participated can be summarized as follows:

- A method was presented for DSC and AFM tests that proved promising as shown in the results.
- Temperature scan of −80 °C to 140 °C should cover thermal transition phenomena present in bitumen.
- From the DSC tests conducted here by seven labs it was shown that synthetic wax did not change the glass transition, T_g value of bitumen. However the tests were on one type of bitumen and one type of synthetic wax and at a single concentration level. For more conclusive results more comprehensive studies are recommended.
- Different crude origins might result in different T_g values for bitumen.
- Analysis of T_g seems influenced by the melting range of natural wax (when present) due to overlap in T_g temperature and cold crystallization.
- Conditioning of bitumen at 25 °C is in the melting range of natural wax. Influence of conditioning at 25 °C on total enthalpy is low, but there is an influence in the melting temperatures. This influence can be significant as seen by others [22].
- T_g temperatures obtained from the heating scans are more reproducible and easier to record in comparison to the cooling scans and therefore it is suggested to use T_g's from the heating scans.
- No significant difference was noted for T_g's obtained from the first or second heating scans.
- Enthalpies of crystallization are smaller compared to melting enthalpies derived from the heating scan. The reproducibility on the enthalpies from heating scans was generally better compared to those from cooling scans.
- Larger variations in melting temperature (T_{pm}) were observed between labs in comparison to T_g.
- Using AFM three phases in the materials with wax could be distinguished by different response in phase contrast imaging mode. The contrast displayed depends on imaging parameters and the type of bitumen.
- From the round robin results of three labs using AFM the same phase behavior was observed when the conditioning and sample preparation was held constant.
- The change in the phases with increase in temperature was correlated with the DSC curve and from this it could be concluded that the behavior and appearance of the microstructure is very much related to the wax behavior. Therefore, this research confirms that the so called "Bee" structures are indeed wax induced.

Acknowledgments The authors would like to thank the members of RILEM technical committee 231-NBM for their cooperation and input and Nynas and Q8 for supplying the materials. The contribution of W. Grimes, T. Pauly, F. Turner and J. Forney at WRI, P. Izdebski and B. Fischer and C. Walder from Empa, P. Wedin from Nynas, C. Nijssen-Wester from KPR&T and C. Petiteau from IFSTTAR is greatly appreciated.

References

1. ISO 11357-1 Plastics-Differential scanning calorimetry, DSC (2009)
2. ASTM 1356-08 Standard Test Method for Assignment of the Glass Transition Temperatures by Differential Scanning Calorimetry
3. ASTM D 3418-12 Standard Test Method for Transition Temperatures and Enthalpies of Fusion and Crystallization of Polymers by Differential Scanning Calorimetry

4. Loeber L, Sutton O, Morel J, Valleton J-M, Muller G (1996) New direct observations of asphalts and asphalt binders by scanning electron microscopy and atomic force microscopy. J Microsc 182(1):32–39
5. Pauli AT, Grimes RW, Beemer AG, Turner TF, Branthaver JF (2011) Morphology of asphalts, asphalt fractions and model wax-doped asphalts studied by atomic force microscopy. Int J Pavement Eng 12(4):291–309
6. Schmets A, Kringos N, Pauli T, Redelius P, Scarpas T (2010) On the existence of wax-induced phase separation in bitumen. Int J Pavement Eng 11(6):555–563
7. Fischer H, Poulikakos LD, Planche J-P, Das P, Grenfell J (2013) Challenges while performing AFM on Bitumen Proceedings International RILEM Symposium on Multi-Scale Modeling and Characterization of Infrastructure Materials Stockholm 2013
8. Masson J-F, Leblond V, Margeson J (2006) Bitumen morphologies by phase-detection atomic force microscopy. J Microsc 221(1):17–29
9. Masson J-F, Leblond V, Margeson J, Bundalo-Perc S (2007) Low-temperature bitumen stiffness and viscous paraffinic nano- and micro-domains by cryogenic AFM and PDM. J Microsc 227(Part 3):191–202
10. Jäger A, Lackner R, Eisenmenger-Sittner Ch, And Blab R (2004) Identification of four material phases in bitumen by atomic force microscopy. Road Mater Pavement Des (EATA) 5:9–24
11. Das PK, Kringos N, Wallqvist V, Birgisson B (2013) Micromechanical investigation of phase separation in bitumen by combining AFM with DSC results. Road Mater Pavement Des 14(S1):25–37
12. Lu X, Langton M, Olofsson P, Redelius P (2005) Wax morphology in bitumen. J Mater Sci 40(8):1893–1900
13. Lu X, Redelius P (2007) Effect of bitumen wax on asphalt mixture performance. Constr Build Mater 21(11): 1961–1970
14. Planche JP, Claudy PM, Létoffé JM, Martin D (1998) Using thermal analysis methods to better understand asphalt rheology. Thermochim Acta 324(1–2):223–227
15. Lu X, Redelius P (2006) Compositional and structural characterization of waxes isolated from bitumens. Energy Fuels 20(2):653–660
16. Michon LC, Netzel DA, Turner TF, Martin D, Planche J-P (1999) A 13C NMR and DSC study of the amorphous and crystalline phases in asphalts. Energy Fuels 13(3):602–610
17. Musser BJ, Kilpatrick PK (1998) Molecular characterization of wax isolated from a variety of crude oils. Energy Fuels 12:715–725
18. European Standard EN 12606-1. Bitumen and bituminous binders-determination of the paraffin wax content-part 1:method by distillation
19. ASTM D3418-12 Standard Test Method for Transition Temperatures and Enthalpies of Fusion and Crystallization of Polymers by Differential Scanning Calorimetry
20. Fischer HR, Dillingh EC, Hermse CGM (2012) On the interfacial interaction between bituminous binders and mineral surfaces as present in asphalt mixtures, Appl Surf Sci. ISSN 0169-4332, 10.1016/j.apsusc.2012.11.034
21. Soenen H, Besamusca J, Poulikakos LD, Planche, J-P, Das P, Grenfell J, Chailleux E (2013) Differential Scanning Calorimetry applied to bitumen: Results of the RILEM NBM TG1 Round Robin test. Proceedings International RILEM Symposium on Multi-Scale Modeling and Characterization of Infrastructure Materials Stockholm 2013
22 Claudy P, Letoffe JM, Rondelez F, Germanaud L, King GN, Planche JP. A new interpretation of time-dependent physical hardening in asphalt based on DSC and Optical thermoanalysis. ACS Fuel preprints, Washington DC, 1992_pp 1408–1426